Comparison of SeaWiFS and MODIS Ocean Color Mesoscale Variability

David M. Glover, Scott C. Doney, and Alisdair W. Tullo
Woods Hole Oceanographic Institution

Abstract

Mesoscale (10 to 300 km, weeks to months) physical variability strongly modulates the structure, biomass, and rates of marine ecosystems and their functioning in the ocean. Physical modulation occurs either directly by turbulent advection and stirring or indirectly by impacts on phytoplankton growth rates and trophic interactions via nutrient enrichment, upwelling/downwelling, and changes of the mixed layer depth and thus mean light field. Here, we extend earlier work (Doney et al., 2003) by quantifying the seasonal and interannual variability in mesoscale biological signals contained within the 13-year SeaWiFS (1998-2010) and 8-year MODIS (2003-2010) chlorophyll-a ocean color data. This poster will review our methods for data processing and structure function analysis of the ocean color data. Then we will present the geographical distribution of the inter-annual variability observed in the two data records. Our results demonstrate the differences in magnitude and similarities in scales of variability between these two sensors. This directly addresses the following issues: the temporal and spatial variability of primary productivity and new production using chlorophyll as a proxy and the intercomparison of two satellite sensors that ostensibly measure the same ocean variable, with the ultimate goal of combining the two time series to create a climate data record. Understanding how well these two sensors map onto each other is critical for evaluating trends observed on climatic time scales and for comparing these findings to higher resolution, coupled ecosystem-ocean general circulation models.

Introduction

In a prior analysis of L3m, 9 km SeaWiFS data, Doney *et al.* (2003) were able to partition the observed variability of retrieved chlorophyll *a* into long term, large spatial scale and a short term, short spatial scale components. Here we present a retrospective analysis and comparison of the extant ocean color estimates of chlorophyll from both SeaWiFS (13 years) and MODIS (8 years) instruments.

Methods

The satellite data are processed in the following order:

1. Daily 9km SeaWiFS (R2010.0) or MODIS (R2010.0) chl_a and MODIS SST HDF formatted files are ingested from NASA GSFC.
2. Daily 9km chl_a data are low pass filtered with a Gaussian 200 km kernel.
3. From the low pass filtered daily images a 31-day, Hamming windowed, moving mean is produced for each day.
4. Each daily field has its corresponding 31-day, low pass filtered, windowed, moving mean subtracted to produce daily residual fields.
5. The residual data is further filtered by applying Chauvenet's criterion to each 5° by 5° sub-region to reduce speckling effects of clouds and aerosols.

Below shows six panels for both SeaWiFS and MODIS chlorophyll exhibiting the stages decomposing satellite imagery into low frequency (scales greater than 200 km and one month) and high frequency (scales less than 200 km and one month) variability.

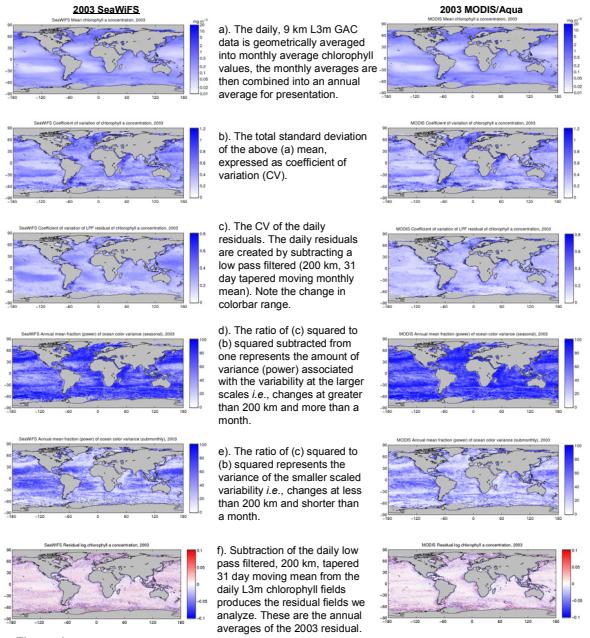

a). The daily, 9 km L3m GAC data is geometrically averaged into monthly average chlorophyll values, the monthly averages are then combined into an annual average for presentation.

b). The total standard deviation of the above (a) mean, expressed as coefficient of variation (CV).

c). The CV of the daily residuals. The daily residuals are created by subtracting a low pass filtered (200 km, 31 day tapered moving monthly mean). Note the change in colorbar range.

d). The ratio of (c) squared to (b) squared subtracted from one represents the amount of variance (power) associated with the variability at the larger scales *i.e.*, changes at greater than 200 km and more than a month.

e). The ratio of (c) squared to (b) squared represents the variance of the smaller scaled variability *i.e.*, changes at less than 200 km and shorter than a month.

f). Subtraction of the daily low pass filtered, 200 km, tapered 31 day moving mean from the daily L3m chlorophyll fields produces the residual fields we analyze. These are the annual averages of the 2003 residual.

Figure 1

Now that SeaWiFS and MODIS are processed with the same software (R2010.0) we can say more about the subtle differences seen above in terms of instrument and not algorithm dependencies.

Geostatistics

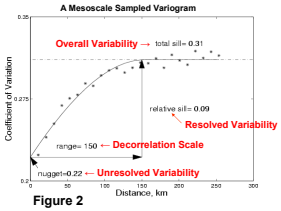

Figure 2

The daily residuals are divided into 5° cells and an empirical two-dimensional variogram is computed for each one using the methods of Marcotte (1996). One-dimensional variograms are extracted in the North-South and East-West directions.

Empirical Semivariance: $\gamma(\vec{v}) = \frac{\sum[Z(\vec{x}) - Z(\vec{x}+\vec{v})]^2}{2N(\vec{v})}$ (1) Z = regionalized variable

The semivariogram or structure function $\gamma(\vec{v})$ measures the local spatial variation of geophysical data $Z(\vec{x})$, describing how samples are related with vector distance $\vec{v}$ (Chilès and Delfiner, 1999) as in Eqn (1). The semivariogram is closely related to the covariance function. In general, two neighboring points are more likely to have similar values than sample pairs farther apart. Thus the semivariogram (covariance) function will have low (high) values at small spatial lags, increasing (decreasing) with distance. Beyond some distance, the data points can often be assumed to be uncorrelated or independent, in which case the semivariogram approaches a uniform variance while the covariance function goes to zero.

A spherical model variogram curve (Eqn 2) is non-linear least square fit to the extracted 1-D semivariances (Fig. 2) and used to derive the variogram parameters shown in Figs. 3-6.

$$\gamma(d) = c_0 + (c_\infty - c_0)\left[\frac{3}{2}\frac{d}{a} - \frac{1}{3}\frac{d^3}{a^3}\right] \quad (2)$$

- c_0 unresolved variability (nugget)
- c_∞ total variability (sill, variance)
- a decorrelation length (range)
- d lag between points
- γ extracted semivariances

Results

The global distributions of the geostatistical parameters are presented here for the year 2003 (first year with complete overlap between SeaWiFS and MODIS/A) for the East-West direction only. The nugget, sill and relative sill are presented in units of coefficient of variability (CV), ranges are in kilometers.

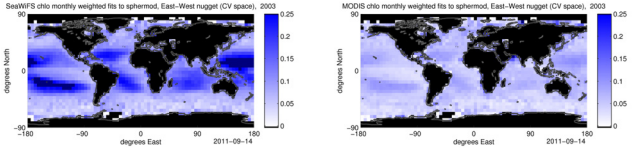

Figure 3 Unresolved variability: Represents variability occurring on scales smaller than the pixels (9 km) and variability due to geophysical or algorithmic noise. SeaWiFS has higher levels of this variability than MODIS/A.

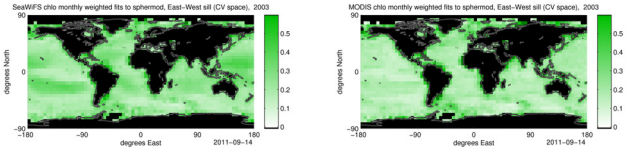

Figure 4 Total variability: is greater for SeaWiFS than MODIS, particularly (as noted in Doney et al., 2003) in the oligotrophic gyre regions.

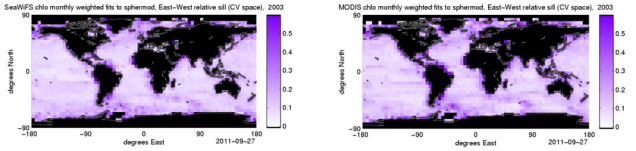

Figure 5 Resolved variability: Total variability (Fig. 4) minus unresolved variability (Fig. 3) yields the resolved variability, the variations that can be seen with the space and time resolution of the data being analyzed. Although similar in appearance, the differences are important (see Fig. 9).

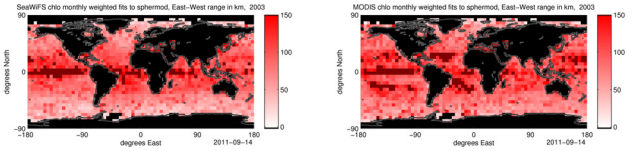

Figure 6 Decorrelation scales: The decorrelation scale is an estimate of the distance between two data points (pixels) when they become statistically uncorrelated.

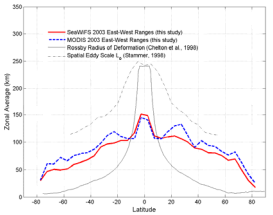

Figure 7: Zonal averages of the east-west ranges from SeaWiFS (heavy red line), MODIS/A (heavy dashed blue line), the Rossby Radius of Deformation (thin solid line) computed from Chelton et al. [1998], and the spatial eddy scale (L_0) from the first zero-crossing of the alongtrack autocorrelation function of TOPEX/Poseidon SSH (thin dot-dashed line) [Stammer, 1997].

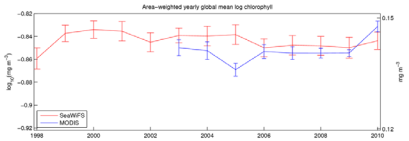

Figure 8: The area-weighted, annual mean chlorophyll in $\log_{10}$(mg Chl m^{-3}) for the entire extant time series of both instruments (±std error of the mean). Although we present geometric means, we find results similar to those of Gregg and Casey (2010). Further we find little immediate evidence of a long term, decreasing trend in the historic satellite data (Boyce et al., 2010).

Figure 9: However, when we examine the area-weighted, annual mean geostatistical parameters (in both East-West and North-South directions) we find otherwise. SeaWiFS has a greater amount of total and unresolved variability, but when the resolved variability is computed MODIS has the higher values. Additionally, while the North-South decorrelation scales are approximately the same for the two instruments, MODIS has slightly longer scales in East-West directions.

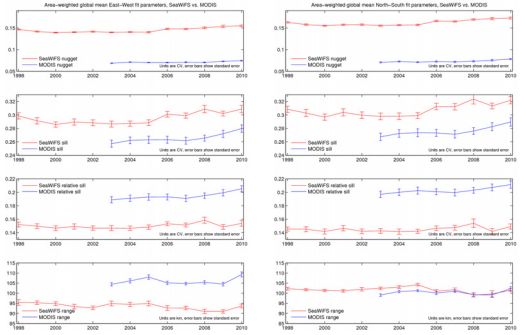

References

Boyce, D.G., M.R. Lewis, and B. Worm, 2010, Global phytoplankton decline over the past century, *Nature*, **466**, 591-596, doi 10.1038/nature09268.

Chelton, D. B., R. A. deSzoeke, M. G. Schlax, K. E. Naggar, and N. Siwertz, Geographical variability of the first baroclinic Rossby radius of deformation, J. Phys. Oceanogr., 28, 433–460, 1998.

Chilès, J-P. and P. Delfiner, 1999, *Geostatistics, Modeling Spatial Uncertainty*, Wiley Inter-science series in Probability and Statistics, New York, NY, 695 pp.

Doney, S.C., D.M. Glover, S.J. McCue, and M. Fuentes, 2003, Mesoscale variability of Sea-viewing Wide Field-of-view Sensor (SeaWiFS) satellite ocean color: Global patterns and spatial scales, *J. Geophys. Res.*, **108**(C2), 3024, doi:10.1029/2001JC000843.

Gregg, W.W. and N.W. Casey, 2010, Improving the consistency of ocean color data: A step toward climate data records, *Geophys. Res. Lett.*,**37**, L04605, doi:10.1029/2009GL041893

Marcotte, D. 1996, Fast variogram computation with FFT, *Computers and Geosciences*, **22**(10), 1175-1186.

Stammer, D., Global characteristics of ocean variability estimated from regional TOPEX/POSEIDON altimeter measurements, J. Phys. Oceanogr., 27, 1743–1769, 1997.